Pathogens and Disease, 76, 2018, fty082

doi: 10.1093/femspd/fty082
Advance Access Publication Date: 15 November 2018
Research Article

RESEARCH ARTICLE

Listeriolysin O-dependent host surfaceome remodeling modulates *Listeria monocytogenes* invasion

Andreas Kühbacher[1,2,3,†], Karel Novy[4,‡], Juan J. Quereda[1,2,3,§], Martin Sachse[5], Maryse Moya-Nilges[5], Bernd Wollscheid[4], Pascale Cossart[1,2,3] and Javier Pizarro-Cerdá[1,2,3,6,*]

[1]Institut Pasteur, Unité des Interactions Bactéries Cellules, Paris F-75015, France, [2]INSERM, U604, Paris F-75015, France, [3]INRA, USC2020, Paris F-75015, France, [4]Institute of Molecular Systems Biology and Department of Health Sciences and Technology, ETH Zürich, Otto-Stern-Weg 3, 8093 Zürich, Switzerland, [5]Institut Pasteur, UTechS Ultrastructural BioImaging, Paris F-75015, France and [6]Institut Pasteur, Unité de Recherche Yersinia, Paris F-75015, France

[*]**Corresponding author:** Institut Pasteur, Unité de Recherche *Yersinia*, 28 rue du Docteur Roux, 75015 Paris, France; Tel: 3314568 8326; Fax: 331 4568 8954; E-mail : pizarroj@pasteur.fr
One sentence summary: Host surfaceome remodeling modulates Listeria infection
Editor: Michel Popoff

[†]Current address: Farco-Pharma GmbH, Im Mediapark 8a, 50670 Cologne, Germany
[‡]Current address: Biognosys AG, Wagistrasse 21, 8952 Schlieren, Switzerland
[§]Current address: Grupo Fisiopatología de la Reproducción, Departamento Producción y Sanidad Animal, Salud Publica Veterinaria y Ciencia y Tecnología de los Alimentos, Facultad de Veterinaria, Universidad Cardenal Herrera-CEU, CEU Universities, Valencia, Spain

ABSTRACT

Listeria monocytogenes is a pathogenic bacterium that invades epithelial cells by activating host signaling cascades, which promote bacterial engulfment within a phagosome. The pore-forming toxin listeriolysin O (LLO), which is required for bacteria phagosomal escape, has also been associated with the activation of several signaling pathways when secreted by extracellular bacteria, including Ca^{2+} influx and promotion of *L. monocytogenes* entry. Quantitative host surfaceome analysis revealed significant quantitative remodeling of a defined set of cell surface glycoproteins upon LLO treatment, including a subset previously identified to play a role in the *L. monocytogenes* infection process. Our data further shows that the lysosomal-associated membrane proteins LAMP-1 and LAMP-2 are translocated to the cellular surface and those LLO-induced Ca^{2+} fluxes are required to trigger the surface relocalization of LAMP-1. Finally, we identify late endosomes/lysosomes as the major donor compartments of LAMP-1 upon LLO treatment and by perturbing their function, we suggest that these organelles participate in *L. monocytogenes* invasion.

Keywords: pore-forming toxin; late endosomes; lysosomes; lysosomal-associated membrane protein 1

INTRODUCTION

Listeria monocytogenes is a Gram-positive bacterium responsible for listeriosis, a food-borne disease characterized by gastroenteritis and bacteremia in immuno-compromised individuals, meningitis in the new-born and abortion in pregnant women (Lecuit 2007; Swaminathan and Gerner-Smidt 2007).

Received: 12 September 2018; **Accepted:** 13 November 2018

Listeria monocytogenes pathogenicity relies on its ability to cross several host tissue barriers including the intestine, the placenta and the blood-brain barrier, and to survive within macrophages as well as to invade and replicate in epithelial cells (Pizarro-Cerdá, Kühbacher and Cossart 2012; Pizarro-Cerdá *et al.* 2016). Cellular invasion requires the presence of the bacterial surface proteins internalin (InlA) and/or InlB and their interaction with the cellular receptors E-cadherin and/or Met, respectively (Gaillard *et al.* 1991; Mengaud *et al.* 1996; Shen *et al.* 2000; Gessain *et al.* 2015; Quereda *et al.* 2018). Activation of host cell receptors leads to recruitment of a clathrin-based internalization machinery that promotes actin polymerization and plasma membrane rearrangements orchestrating bacterial engulfment (Pizarro-Cerdá and Cossart 2009; Pizarro-Cerdá, Bonazzi and Cossart 2010; Bonazzi *et al.* 2012). Following cellular invasion, *L. monocytogenes* disrupts its internalization compartment through the action of the pore-forming toxin listeriolysin O (LLO), leading to bacterial escape to the host cell cytoplasm (Quereda, Cossart and Pizarro-Cerdá 2016). Cytoplasmic bacteria, through the activity of the surface protein ActA, promote their own movement via an actin-based motility system that leads to cell-to-cell spread (Gouin, Welch and Cossart 2005; Van Troys *et al.* 2008).

Bacterial invasion of non-polarized epithelial cells by means of the InlB-dependent internalization pathway is a complex process that requires interaction of many molecular partners. Met is a receptor tyrosine kinase that upon interaction with InlB promotes its own phosphorylation and that of the molecular adaptors Cbl, Gab1 and Shc, which are involved in the recruitment of a type I PI 3-kinase to bacterial entry sites (Ireton *et al.* 1996; Ireton, Payrastre and Cossart 1999). Phosphatidylinositol(3,4,5)P_3 produced by the PI 3-kinase is redistributed in lipid rafts and is required for Rac activation (Seveau 2004; Seveau *et al.* 2007; Pizarro-Cerdá, Kühbacher and Cossart 2014; Gessain *et al.* 2015). Downstream of Rac, several WASP-related proteins promote actin polymerization by the Arp2/3 complex while ENA/Vasp favor actin filament elongation (Bierne *et al.* 2005). The actin depolymerization process is also highly regulated at bacterial entry sites (Kühbacher *et al.* 2012) and disassembly of an actin-rich phagocytic cup is required for cell invasion (Bierne *et al.* 2001). In parallel, Cbl ubiquitinates Met through its ubiquitin-ligase activity and therefore favors the recruitment to *L. monocytogenes* invasion foci of a clathrin-associated machinery that promotes additional actin polymerization (Veiga and Cossart 2005; Veiga *et al.* 2007; Bonazzi *et al.* 2011).

Besides InlB, ActA and LLO have been reported to foster cellular invasion by *L. monocytogenes* in epithelial cells (Suárez *et al.* 2001; Dramsi and Cossart 2003; Vadia *et al.* 2011). In particular, LLO is a secreted pleiotropic bacterial effector that acts extracellularly on host plasma membranes by promoting Ca^{2+} influx in target cells (Dramsi and Cossart 2003), modulating mitochondrial dynamics (Stavru and Cossart 2011; Stavru *et al.* 2013), perturbing the telomerase function (Samba-Louaka, Stavru and Cossart 2012), inducing histone post-translational modifications (Hamon *et al.* 2007; Hamon and Cossart 2011) and impairing host cell protein sumoylation (Ribet *et al.* 2010; Malet *et al.* 2018). Using a quantitative chemoproteomic strategy (Wollscheid *et al.* 2009; Hofmann, Bausch-Fluck and Wollscheid 2013), we assessed the impact of LLO exposure on the host cell surface exposed N-glycoproteins, here referred as surfaceome. Cross-correlation of these results with functional data from a previous genome-wide siRNA screen for *L. monocytogenes* infection (Kühbacher *et al.* 2015) revealed key molecular players that positively or negatively affect bacterial infection. We show in particular that LLO promotes fusion of late endosomal compartments with the plasma membrane at bacterial entry foci and participates in efficient *L. monocytogenes* invasion of host cells.

MATERIALS AND METHODS

Cell culture and bacteria

HeLa CCL-2 cells from the American Type Culture Collection were cultured at 37°C in DMEM supplemented with 10% fetal calf serum (FCS) in a humidified 10% CO_2 atmosphere. *Listeria monocytogenes* strain EGDe.PrfA* was cultured in brain heart infusion at 37°C. For infection experiments, bacteria were grown for 3 to 5 h in order to obtain cultures in logarithmic phase or overnight to reach the stationary phase. One ml of bacteria culture was washed three times with 1 ml PBS, the OD at 600 nm was measured to calculate the bacteria number and cells were infected in DMEM at a multiplicity of infection of 25 to 50 bacteria per cell (Pizarro-Cerdá, Lecuit and Cossart 2002; Kühbacher, Cossart and Pizarro-Cerdá 2014). To synchronize infection, bacteria were centrifuged on cells for 5 min at 1000 rpm at room temperature. For treatment of cells with purified LLO, cells were starved for at least 3 h with DMEM. Purified LLO was diluted in DMEM at indicated concentrations.

Probes, recombinant proteins and drugs

EGTA, horseradish peroxidase (HRP), H_2O_2, triton X-100, saponin and 3,3′-Diaminobenzidine tetrahydrochloride (DAB) were purchased from Sigma. Recombinant LLO and LLO^{w492A} were produced as previously described (Pizarro-Cerdá, Lecuit and Cossart 2002; Glomski, Decatur and Portnoy 2003).

Plasmid transfection

Transfection with a plasmid coding for canine EGFP-LAMP-1 (described in Lozach *et al.* 2011) was performed 24 h prior to assays using the FuGENE HD transfection procedure (Roche Applied Science) according to the manufacturers protocol. The final plasmid concentration was 0.5 μg/ml.

Flow cytometry

Cells were infected or treated with recombinant proteins at 37°C for indicated times. Subsequently cells were detached for 5 min at 37°C using calcium and magnesium free PBS supplemented with 0.5mM EDTA. Cells were then fixed for 20 min with 4% paraformaldehyde (PFA) in PBS on ice and stained for surface LAMP-1 or LAMP-2 or treated with isotype antibody for 1h in PBS supplemented with 1% bovine serum albumin (BSA). Fluorescently labeled Antibodies (anti-LAMP-1-Phycoerythrin 555801, anti-LAMP-2-FITC 560946 and mouse isotype control IgG-Phycoerythrin 555749 (BD Bioscience)) were diluted according to the manufacturers recommendations. For staining of total LAMP-1 0.05% saponin was added to the staining solution. Fluorescent signals were measured using a FACSCalibur flow cytometer (BD Biosciences). Dead cells were excluded by gating.

Hexosaminidase assay

To measure the release of lysosomal hexosaminidase, cells in 96 well plates were stimulated by infection or treatment with recombinant LLO for 20 min in DMEM without phenol red.

87.5 μl of supernatants were then transferred to a new 96 well plate. The rest of the supernatant was aspirated and the cells were lysed for 15 min at 37°C by addition of 100 μl PBS supplemented with 0.1% Triton X-100. Lysates were then diluted 1:10 and 87.5 μl were transferred to a new 96 well plate. 87.5 μl PBS was added to blank wells. 12.5 μl of 6 mM 4-methyl-umbellyferyl-N-acetylb-d-glucosaminide (69 585, Sigma) in citrate-phosphate buffer, pH 4.5 was added to each well and after incubation for 15 min at 37°C the reaction was stopped by addition of 25 μl 2 M Na_2CO_3 and 1.1 M glycine. Fluorescence at 450 nm was measured after excitation at 365 nm using a spectrofluorometer (Flx-Xenius, Safas).

Immunofluorescence staining and live-cell imaging

For immunofluorescence staining 50 000 cells were seeded on 12 mm round glass coverslips in 24 well plates the day before the experiment. After fixation with 4% PFA, cells were stained with a Phycoerythrin coupled antibody against LAMP-1 for 40 min in staining solution (PBS, 1% BSA, 0.05% saponin). For labeling of extracellular LAMP-1, staining solution without saponin was used. Differential bacteria staining was carried out by first staining extracellular bacteria with a rabbit-derived antibody (R11) and a secondary Alexa Fluor 488-coupled antibody (Molecular Probes) both for 30 min in staining solution without saponin followed by thorough washes and staining of total bacteria with DAPI or with R11 and a secondary Alexa Fluor 350- or Cy3-coupled antibody. Coverslips were mounted on microscopy glass slides with Fluoromount (Interchim) and images were acquired with a 63x or 100x objective installed on an inverted wide-field fluorescence microscope (Axiovert 200M, Carl Zeiss Microscopy), equipped with an EMCCD camera (Neo, Andor) and the imaging software MetaMorph (Molecular Devices). For live-cell imaging, 200 000 cells were seeded and transfected with a plasmid coding for canine LAMP-1-GFP the day before in 35mm glass bottom dishes (Mattek). For infections and image acquisition medium was replaced by DMEM without phenol red. Infections were synchronized by centrifugation for 5min at 1000 rpm before imaging. Images were acquired with a 37°C pre-warmed microscope (Axiobserver Z1, Zeiss) equipped with an EMCCD camera (Evolve, Photometrics), a spinning disk head (CSU X-1, Yokogawa) and a laser launch system (405, 491, 546 and 642 nm, Photometrics) in a 5% CO_2-containing atmosphere. Images were taken every 5 to 20 sec. For imaging of LLO-treated cells, 1 nm LLO was added during image acquisition as indicated in the corresponding figure.

Exosome purification

For each condition, three 125 cm^2 cell culture flasks with 70% to 90% confluent HeLa cells were prepared. Before treatment with mock DMEM or 1 nM LLO in DMEM for 20 min, cells were starved in DMEM for 3 h. Supernatants of treated cells were collected and centrifuged first at 2000 rcf for 20 min, supernatants were again transferred to new tubes and centrifuged at 10 000 rcf for another 30 min to remove cell debris. Cleared supernatants were centrifuged at 100 000 rcf for 70 min to concentrate the exosome fraction which was then washed by removal of the supernatant, re-suspension in PBS and repetition of the previous centrifugation step. The washed exosome fraction was kept at –80°C as aliquotes of 25 μl. For fluorescent detection of exosomes, purified fractions were seeded on glass coverslips and fixed with 4% PFA. Exosomes were then stained for CD63 with a mouse-anti-CD63 antibody TS63 and a secondary Alexa Fluor 488-coupled antibody.

Lysosome/late endosome quenching

To inactivate late endocytic compartments, the endocytic pathway was loaded with HRP by treatment with DMEM, supplemented with 1% BSA and 5 mg/ml HRP for 1.5 h at 37°C before washout of HRP three times with Ca^{2+} and Mg^{2+} containing PBS and a chase for 30 min at 37°C in DMEM, supplemented with 1% BSA to allow the HRP to accumulate in late endocytic compartments and be cleared from the early endocytic pathway. Cells were then transferred to ice and treated with 100 μg/ml DAB and 0.0025 % H_2O_2 in Ca^{2+} and Mg^{2+} containing PBS for another 30 min. After washing three times with PBS and once with DMEM cells were transferred again to 37°C for 5 min and then immediately infected or treated with LLO.

Cell Surface Capture technology

HeLa cells were expanded on 14 cm dishes in DMEM supplemented with 10% FCS and 4 mM L-Glutamine. Cells were starved overnight in DMEM at 37°C and then treated for 20 min with purified LLO at a concentration 1 nM. Control cells were incubated in DMEM at 37°C for 20 min. Cell surface proteins were captured using the cell surface capture (CSC) technology as described elsewhere (Wollscheid *et al.* 2009; Hofmann, Bausch-Fluck and Wollscheid 2013). Briefly, cells were washed on plates twice in ice-cold PBS then in ice-cold PBS pH 6.5 and oxidized in PBS pH 6.5 supplemented with 2 mM sodium meta-periodate for 15 min at 4°C. The oxidized cells were washed with PBS pH 6.5, biocytin hydrazide was added to a final concentration of 77 μM in PBS pH 6.5 and incubated at 4°C for 1h. After washing in PBS, cells were scraped and resuspended in 50 mM ammonium bicarbonate and lysed by sonication. Nuclei were pelleted and the supernatant collected. Rapigest was added to a final concentration of 0.1% and the solution was sonicated for 3 min. The proteins were reduced with 5 mM Tris(2-carboxyethyl)phosphine and alkylated with 10 mM iodoacetamide. Proteins were enzymatically digested overnight with trypsin at a substrate:enzyme ratio of 50:1. After trypsin heat inactivation, streptavidin beads were added to the peptides and incubated for 2 h at room temperature. The beads were washed with 5 M sodium chloride, triton X-100 based buffer, 50 mM ammonium bicarbonate, 100 mM sodium bicarbonate adjusted to pH 11 and finally with 50 mM ammonium bicarbonate. Peptide-N-glycosidase F was added to the beads and incubated overnight at 37°C. Released peptides were desalted on a C18-column and separated by reversed-phase chromatography on a high-performance liquid chromatography (HPLC) column (75-μm inner diameter, New Objective) that was packed in-house with a 10-cm stationary phase (Magic C18AQ, 200 Å, 3 micron Michrom Bioresources) and connected to a nano-flow HPLC combined with an autosampler (EASY-nLC II, Proxeon). The HPLC was coupled to a LTQ-Orbitrap XL mass spectrometer (Thermo Scientific) equipped with a nanoelectrospray ion source (Thermo Scientific). Peptides were loaded onto the column with 99.9% buffer A (99.9% H2O, 0.1% FA) and eluted with 300 nl/min over a 60-min linear gradient from 7%–35% buffer B (99.9% ACN, 0.1% FA). After the gradient, the column was washed with 80% buffer B and re-equilibrated with buffer A. Mass spectra were acquired in a data-dependent manner, with an automatic switch between MS and MS/MS scans. High- resolution MS scans were acquired in the Orbitrap (60 000 FWHM, target value 106) to monitor peptide ions in the mass range of

300–1600 m/z, followed by collision-induced dissociation MS/MS scans in the ion trap (minimum signal threshold 250, target value 104, isolation width 2 m/z) of the five most intense precursor ions. To avoid multiple scans of dominant ions, the precursor ion masses of scanned ions were dynamically excluded from MS/MS analysis for 30 s. Singly charged ions and ions with unassigned charge states were excluded from MS/MS fragmentation. RAW files were converted into the open mzXML format and searched by the SEQUEST (Eng, McCormack and Yates 1994) search engine against the UniProt/Swiss-Prot database (v57.15 of *H. sapiens* and *L. monocytogenes*) concatenated with common contaminants. Search parameters for the peptide identification included a precursor mass tolerance of 0.05 Da, a minimum of one tryptic terminus and a maximum of two internal tryptic missed cleavage sites. Cysteine carbamidomethylation (+ 57.021 Da) was set as a static amino acid modification and methionine oxidation (+15.995 Da) as well as asparagine deamidation (+ 0.9840 Da) were set as variable modifications. The PeptideProphet and ProteinProphet tools of the Trans-Proteomic Pipeline (Keller *et al.* 2005) (TPP version 4.5) were used for the probability scoring of peptides spectrum matches.and protein inference. Protein identifications were filtered to reach an estimated false-discovery rate of ≤1%. Peptide feature intensities were extracted using the Progenesis LC-MS software (Nonlinear Dynamics). Matched peptides were filtered for the presence of the N[115]-X-S/T motif (wherein N[115] stands for a deamidated asparagine residue, X stands for any amino acid except proline and S/T for serine or threonine, respectively). Constant normalization was performed on the log-transformed intensities of peptide features across samples. Relative protein abundance and statistical significance between stimulated and control samples were assessed using the MSstats library (Clough *et al.* 2009) in the statistical software package R.

RESULTS

LLO alters the host surfaceome

LLO pores in the plasma membrane cause ion fluxes between the cytoplasm and the extracellular space that have been associated with increased *L. monocytogenes* cell invasion (Dramsi and Cossart 2003; Stavru and Cossart 2011). In particular, influx of extracellular calcium may induce secretory processes, leading to changes in the surfaceome protein composition. To understand how LLO impacts *L. monocytogenes* cell invasion, we analyzed LLO-dependent changes of the surfaceome composition of HeLa cells using the chemoproteomic CSC enrichment strategy, targeting specifically the cell surface-exposed N-glycoproteins combined with quantitative mass spectrometry-based proteomics (Wollscheid *et al.* 2009; Hofmann, Bausch-Fluck and Wollscheid 2013).

The cell surface abundance of 10 glycoproteins was significantly increased and 20 glycoproteins were significantly decreased at the cell surface after treatment for 20 min with 1 nM LLO (Fig. 1A, labeled proteins in upper quadrants). Out of these 30 glycoproteins (Fig. 1B, black bars in all panels), 24 have been previously studied in a genome-wide siRNA screen for *L monocytogenes* infection (Kühbacher *et al.* 2015) (Fig. 1B, left and center panels). These 24 glycoproteins can be divided in four classes: (i) proteins that inhibit infection (positive infection Z-score) that were increased on the cell surface upon LLO treatment (SLC6A15, EDEM3) (Fig. 1B, left panel), (ii) proteins that are required for infection (negative infection Z-score) that were decreased on the cell surface upon LLO treatment (IL6ST, SLC3A2, FRAS1, AXL, SC29A1, LRRC4C) (Fig. 1B, left panel), (iii) proteins that are required for infection and are increased at the cell surface (NUP210, THY1, LAMP2, HYOU1) (Fig. 1B, center panel) and (iv) proteins that inhibit infection and are decreased at the cell surface (PTGFRN, BST2, CD70, PTPRF, PTK7, BTN2A1, DCBLD1, VASN, IGSF3, ITGA5, SLC1A5, GAPDH) (Fig. 1B, center panel).

The first two classes are comprised of proteins that when combining the translocation phenotype and the infection phenotype most likely result in inhibition of infection (Fig. 1B, left panel) while the latter two classes are expected to promote *L. monocytogenes* infection (Fig. 1B, center panel). Therefore, LLO changes the host surfaceome in two ways: membrane associated proteins that inhibit infection like the amino acid transporter SLC1A5 are depleted in abundance from the cell surface location, while the heat shock protein HYOU1, which was previously shown to be required for *L. monocytogenes* infection (Kühbacher *et al.* 2015) is enriched at the cell surface and the expected outcome in both cases is to promote *L. monocytogenes* invasion (Fig. 1B, center panel). Interestingly, we also observe a strong decrease in the abundance of proteins in the plasma membrane location that, according to our previous siRNA screen results, are highly important for *L. monocytogenes* infection (Fig. 1B, left panel). This is the case, for example for the membrane transporters SLC3A2, SLC29A1 as well as LRRC4C which has been associated with signaling by the receptor tyrosine kinase AXL. Taken together, these results indicate that LLO-dependent cell surface changes can affect positively or negatively *L. monocytogenes* invasion in HeLa cells.

LLO induces translocation of late endosomal compartments to the cell surface

To better understand the cellular functions leading to LLO-dependent changes of the cell surface and modulation of *L. monocytogenes* invasion, we performed a cellular component enrichment analysis using the gene ontology enrichment tool of the STRING database (www.string-db.org) (Szklarczyk *et al.* 2015). This analysis showed that the 10 significantly enriched proteins at the cell surface upon LLO treatment are related to the endoplasmic reticulum (ER) (FKBP9, GLT25D1, NUP210, HYOU1, THY1), to extracellular exosomes (LGAL3BP, LAMP1, LAMP2, HYOU1, THY1) and to late endosomes/lysosomes (LAMP1, LAMP2) (Fig. 2A and 2B).

LLO dependent translocation of the late endosomal/lysosomal membrane protein LAMP-1 was further characterized by fluorescence microscopy, and surface translocation of LAMP-1 could be readily observed as a smooth extracellular staining (Fig. 3A). LLO dependent translocation of the late endosomal/lysosomal membrane proteins LAMP-1 and LAMP-2 was also characterized by flow cytometry: a marked increase of both proteins at the cell surface was detected already as early as 5 min after LLO treatment and afterwards increased only slightly (Fig. 3B, right panel). This process was concentration dependent and up to a 6- and 2-fold increase in the surface levels of LAMP-1 and LAMP-2, respectively, could be observed on cells exposed to 1 nM LLO for 20 min (Fig. 3B, left panel). Cellular treatment with LLO^{w492A} that binds to cells but does not form pores (Michel *et al.* 1990) did not change the localization of LAMP-1 or LAMP-2, confirming that the LLO pore-forming activity is required for the translocation of the lysosomal proteins. In order to follow the dynamics of this translocation, EGFP-LAMP-1-expressing HeLa cells were recorded by live-cell microscopy during LLO-treatment.

(A)

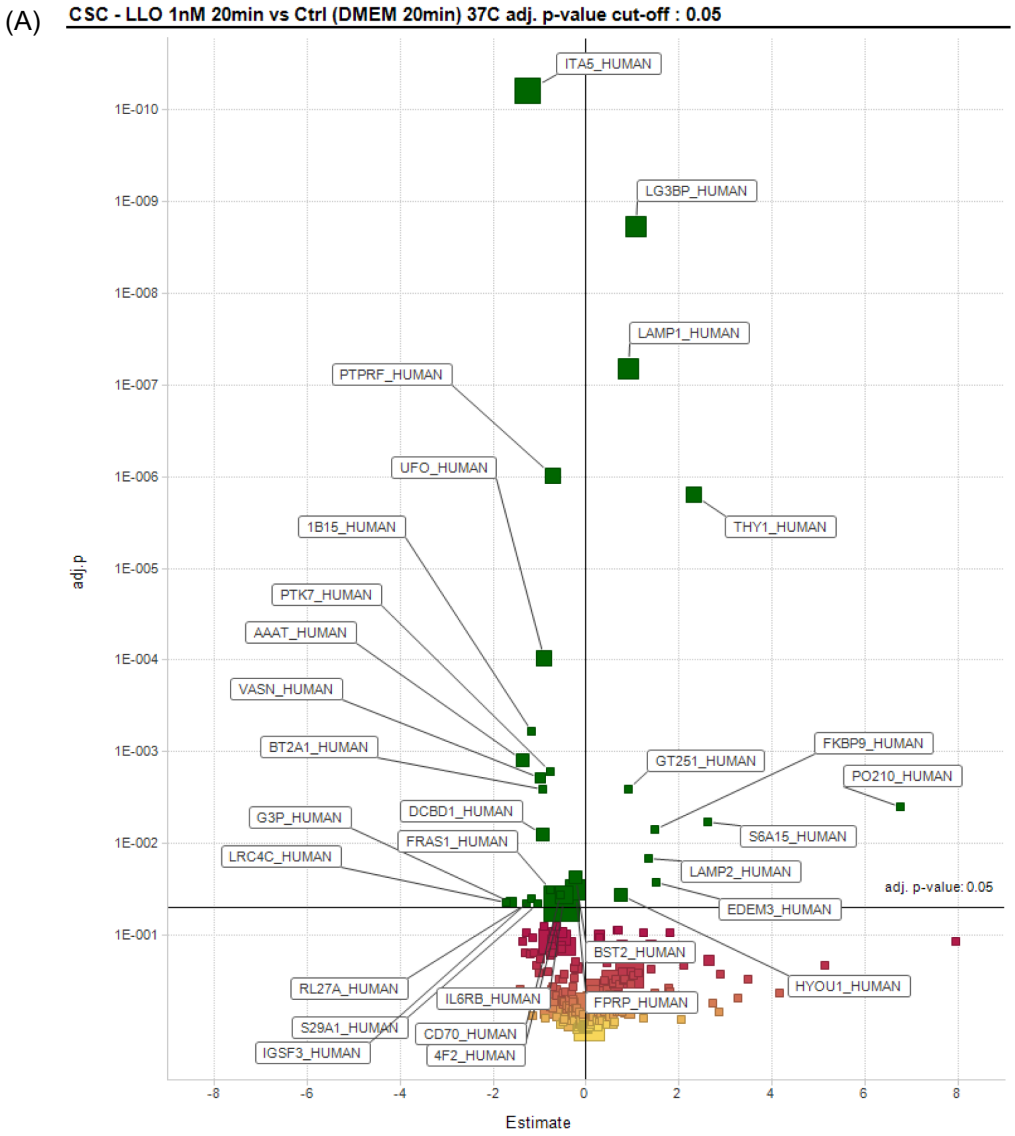
CSC - LLO 1nM 20min vs Ctrl (DMEM 20min) 37C adj. p-value cut-off : 0.05
adj.p
1E-010
1E-009
1E-008
1E-007
1E-006
1E-005
1E-004
1E-003
1E-002
1E-001
ITA5_HUMAN
LG3BP_HUMAN
LAMP1_HUMAN
PTPRF_HUMAN
UFO_HUMAN
THY1_HUMAN
1B15_HUMAN
PTK7_HUMAN
AAAT_HUMAN
VASN_HUMAN
BT2A1_HUMAN
FKBP9_HUMAN
GT251_HUMAN
PO210_HUMAN
G3P_HUMAN
DCBD1_HUMAN
S6A15_HUMAN
FRAS1_HUMAN
LRC4C_HUMAN
LAMP2_HUMAN
adj. p-value: 0.05
EDEM3_HUMAN
BST2_HUMAN
HYOU1_HUMAN
RL27A_HUMAN
IL6RB_HUMAN
FPRP_HUMAN
S29A1_HUMAN
CD70_HUMAN
IGSF3_HUMAN
4F2_HUMAN
-8
-6
-4
-2
0
2
4
6
8
Estimate

(B)

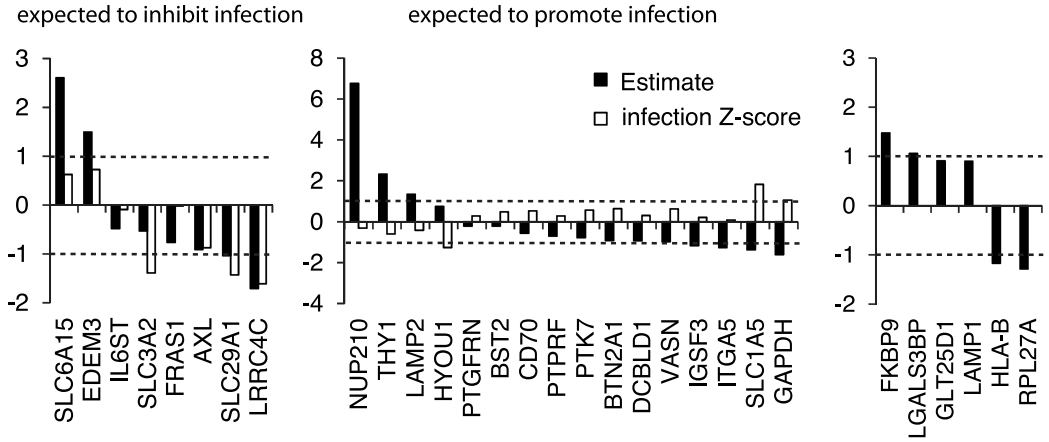
expected to inhibit infection
expected to promote infection
Estimate
infection Z-score
SLC6A15
EDEM3
IL6ST
SLC3A2
FRAS1
AXL
SLC29A1
LRRC4C
NUP210
THY1
LAMP2
HYOU1
PTGFRN
BST2
CD70
PTPRF
PTK7
BTN2A1
DCBLD1
VASN
IGSF3
ITGA5
SLC1A5
GAPDH
FKBP9
LGALS3BP
GLT25D1
LAMP1
HLA-B
RPL27A

Figure 1. Changes of the cell surface proteome after LLO treatment **A**, HeLa cells were treated with 1nM LLO or medium only for 20 min. Subsequently cells were detached and processed for cell surface capturing of glycoproteins followed by mass spectrometry-based proteomics analysis. The log2 fold change and adjusted P-value of differentially changed protein cell surface expression are shown. Tests for differential expression were performed using a linear mixed model and P-values were adjusted using Benjamini and Hochberg method. **B**, Log2 fold change of significantly enriched and depleted proteins at the cell surface (black bars, all panels) and the corresponding Z-score of infection from previously published genome-wide siRNA screens (white bars, left and center panels). Proteins are divided in four categories: (i) increased cell surface enrichment and positive Z-score; (ii) decreased cell surface exposure and negative Z-score; (iii) increased cell surface enrichment and negative Z-score and (iv) decreased cell surface exposure and positive Z-score. The right panel shows molecules which display significant changes at the cell surface distribution but which were not present in our previous siRNA screen. Dotted line: + 1 and -1 Z-score limit.

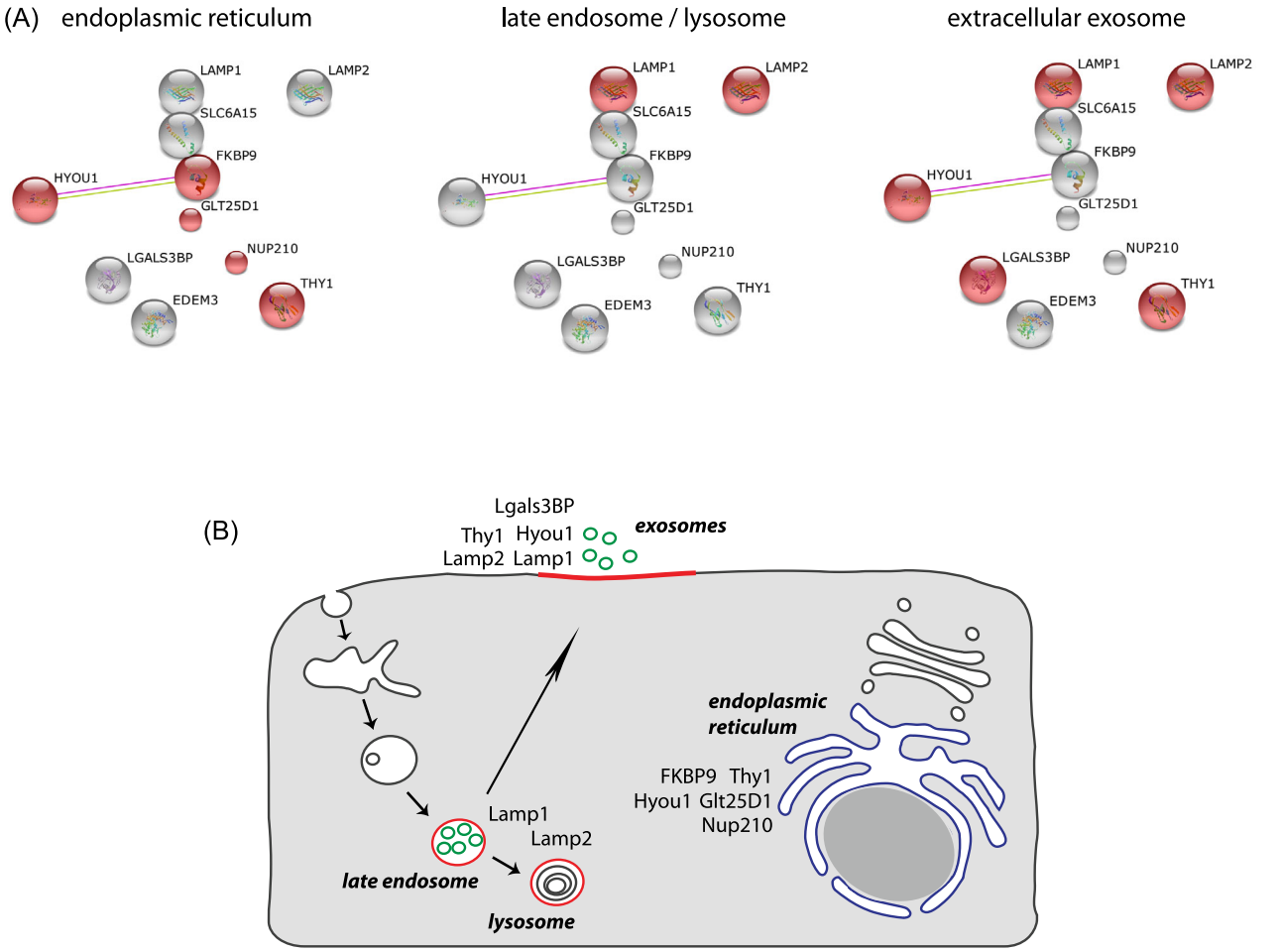

Figure 2. Assignment of translocated proteins to cellular components. **A**, String network (stringency: 0.4) of significantly enriched cell surface proteins upon LLO treatment. Proteins belonging to the indicated cellular components are highlighted in red. **B**, Schematic representation of a human cell indicating the proteins signifcantly enriched at the cell surface upon LLO treatment, and the cellular components to which these proteins are associated.

LLO promoted a major change not only in the dynamic movement of intracellular LAMP-1 positive vesicles but also in the distribution of EGFP-LAMP-1: before LLO treatment, EGFP-LAMP-1 is detectable as bright mobile spots (Fig. 3C); upon treatment, some of these structures disappear (inset, Fig. 3C) and remaining spots become immobile. Together these results suggest that LAMP-1 positive intracellular compartments such as late endosomes or lysosomes are very rapidly translocated to the cell surface upon LLO treatment and that this process is dependent on the pore-forming activity of the toxin. Treatment of cells with EGTA reduced the appearance of EGFP-LAMP1 at the cell surface upon LLO stimulation (Fig. 3D), confirming that Ca^{2+} influx is required for this process. Interestingly, we observed that the *L. monocytogenes* invasion protein InlB synergizes with LLO and also promotes translocation of LAMP-1 and LAMP-2 to the cell surface, although to a much lower extent in comparison to LLO (Supplementary Fig. 1).

If late endocytic compartments fuse with the plasma membrane, luminal lysosomal enzymes are expected to be secreted to the extracellular space. To determine whether *L. monocytogenes* infection promotes the fusion of late endosomes or lysosomes with the plasma membrane, we measured the presence of the luminal lysosomal enzyme β-hexosaminidase in the extracellular space upon cell treatment with LLO. As shown in Fig. 3E, hexosaminidase activity was detected in cell culture medium of cells treated with LLO. Multivesicular late endosomes can fuse with the plasma membrane and release their intraluminal vesicles as structures named exosomes (Stoorvogel *et al.* 2002). We applied an ultracentrifugation-based protocol to purify exosomes and examined preparations from

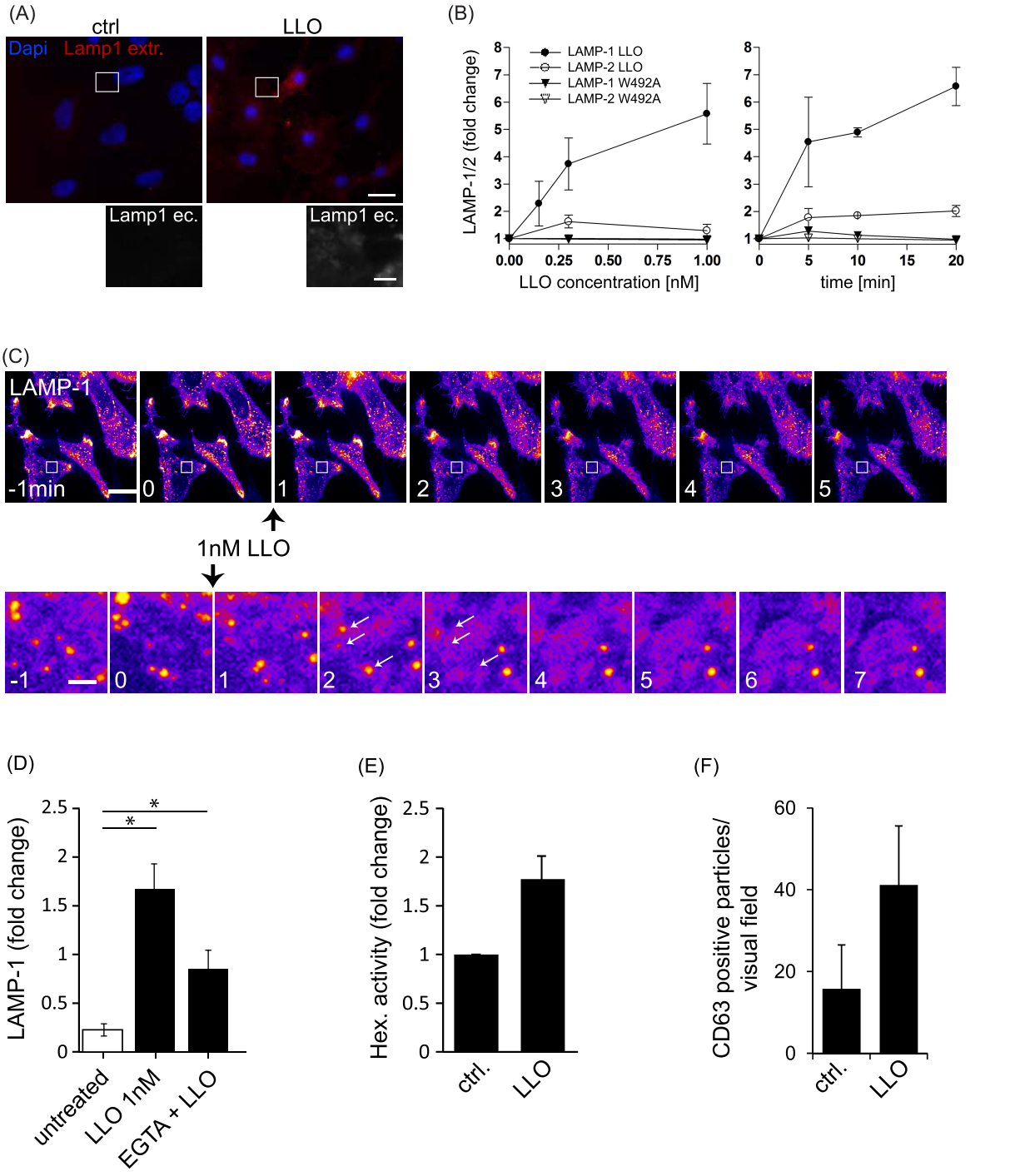

Figure 3. Translocation of late endosomal/lysosomal compartments to the cell surface in response to LLO. **A**, Cells grown on glass coverslips in a 24 well plate were treated for 20 min with 1 nM LLO. Subsequently, cells were fixed and immunostained for extracellular LAMP-1 and for DNA using Dapi after permeabilization Bar: 10 μm (magnification bar: 1 μm). **B**, HeLa cells were treated with 1 nM LLO or LLO^{W492A} (binds to cells but is not able to form pores) for different time intervals (right), or were treated independently with different concentrations of LLO or LLO^{W492A} for 20 min (left). Subsequently, cells were detached, fixed and stained for LAMP-1 or LAMP-2 in the absence of cell permeabilization. Fluorescence was measured by flow cytometry and values are given as fold change of the geometric mean of the fluorescent signal, compared to non-treated cells. Results represent the average of at least three independent experiments + /- standard error of the mean. **C**, HeLa cells transfected with EGFP-LAMP-1 were grown for 24 h in 35 mm imaging dishes. Dishes were then transferred to a 37°C pre-warmed microscope in a 5% CO_2-containing atmosphere and image stacks were taken before and after addition of LLO to a final concentration of 1 nM. The boxed region in the upper panels is enlarged in the lower panels. Bar: 1 μm. **D**, HeLa cells were pretreated for 20 min with 20mM HEPES or 10 mM EGTA and 20mM HEPES and subsequently left untreated or treated for 20 min with 1 nM LLO in the presence of the different pretreatments. Following this, cells were detached, fixed and fluorescently stained for surface accessible LAMP-1 in the absence of permeabilization. The fluorescent signal was measured by flow cytometry. Geometric mean of fluorescence intensity was normalized to the average of all samples. Bars represent the average and geometric mean of three independent experiments (Student's *t*-test: *, $p < 0.05$). **E**, HeLa cells were treated with 1 nM LLO for 20 min and the β-hexosaminidase activity in the cellular supernatant (and cell lysates) was measured fluorometrically. Values represent the fold change of the ratio of β-hexosaminidase activity of supernatants/cell lysates. Results show the average of three independent experiments relative to the mock control + /- SEM. **F**, Exosomes were purified from the supernatant of control and LLO-treated cells by ultracentrifugation, seeded on glass coverslips, fixed, stained for CD63 and quantified by microscopy. Bars represent the mean and standard deviation of six visual fields of a representative experiment.

culture supernatants of control cells versus cells treated with LLO: the exosome preparation from control cells already contains some vesicles with a diameter between 80–150 nm but LAMP-1 positive vesicles/exosomes were only occasionally detected (Supplementary Fig. 2A, I); by contrast, the preparation from LLO-treated cells presented more frequently exosomes displaying a LAMP-1 labeling (Supplementary Fig. 2A, II inset). Isolation and quantification of these compartments by fluorescence microscopy using antibodies against the exosomal marker CD63 confirmed that exosome secretion is highly increased upon cellular exposure to LLO (Fig. 3F). By western blot we also detected higher amounts of CD63 in exosomal fractions isolated from LLO-treated cells (Supplementary Fig. 2B). In conclusion, we determined that LLO treatment leads to the secretion of intracellular compartments of late endosomal nature.

Listeria monocytogenes elicits secretion of late endosomal compartments at invasion foci

During *L. monocytogenes* invasion, the LLO concentration is presumably highest close to the bacterium where the toxin is released. We therefore tested if late endosomes fuse with the host cell plasma membrane at bacterial invasion foci. As shown in Fig. 4A, extracellular LAMP-1 is enriched in the vicinity of bacteria during invasion. Specific fluorescent labeling of extracellular bacteria revealed moreover that endosomal exocytosis at the entry site occurs early during invasion before vacuole closure (Fig. 4B). By spinning disk confocal microscopy, we could follow in living cells the association of EGFP-LAMP-1-positive vesicles with *L. monocytogenes* during the initial steps of cellular invasion (Fig. 4C). As for purified LLO, *L. monocytogenes* induced LAMP-1 translocation to the cell surface was blocked by Ca^{2+} depletion (Fig. 4D).

Applying transmission electron microscopy on *L. monocytogenes* infected cells to investigate the morphological features of the late endosomal compartments that fuse with the plasma membrane upon infection, we detected bacteria within membrane-bound vacuoles that contained small vesicles of 50 to 100 nm diameter (Supplementary Fig. 3A), which correlates with the size of the intraluminal vesicles found in late endosomes (Van Niel *et al.* 2001), indicating an interaction or fusion with these compartments at bacterial entry sites. These results prompted us to investigate whether the unconventional lipid lysobisphosphatidic acid (LBPA), which is particularly detected in intraluminal membranes of late endosomal compartments, could also be found at *L. monocytogenes* entry sites, and by immunofluorescence microscopy LBPA was detected in a subset of bacterial entry foci together with LAMP-1 (Supplementary Fig. 3B). Altogether, these observations suggest that *L. monocytogenes* promotes local exocytosis of late endosomal compartments during cellular invasion before bacterial engulfment is completed.

LLO-dependent secretion of late endosomal compartments at *L. monocytogenes* invasion foci participates in bacterial invasion

To investigate the functional relevance of late endosomal secretion during *L. monocytogenes* cell entry, we first internalized soluble horseradish peroxidase (HRP) in cells for 1.5 h and then performed a chase for 30 min to accumulate HRP in late endosomal compartments (Futter *et al.* 1996). We then perturbed the organization of late endosomes by crosslinking the HRP with 3,3′-diaminobenzidine (DAB): in these conditions, we detected a clear reduction in the surface LAMP-1 levels after LLO treatment (Fig. 5A) or *L. monocytogenes* infection of HeLa cells, (Fig. 5B). We also applied this late endosomal cross-linking procedure and performed invasion assays quantified by differential staining of total and extracellular bacteria: as shown in Fig. 5C, HRP/DAB treatment inhibits cellular invasion by *L. monocytogenes*, suggesting that the delivery of these organelles to the plasma membrane, and in particular to bacterial entry sites, facilitates bacterial internalization.

DISCUSSION

In this work, we assessed host surfaceome protein abundance changes taking place upon cellular exposure to extracellular LLO, and we identify cellular components which can differentially modulate *L. monocytogenes* internalization. In particular, we show that LLO induces the translocation of late endosomal/lysosomal compartments to the bacterial entry foci and that this late endosomal mobilization promotes efficient *L. monocytogenes* invasion of host cells.

We observed a significant downregulation in the abundance of a subset of proteins in the cell surface location, as well as the translocation of proteins from intracellular compartments to the cell surface. Cross-correlation of these results with those of a previous genome-wide siRNA screen to investigate *L. monocytogenes* infection led to the discovery of proteins like the amino acid transporters SLC3A2 and SLC29A1, the receptor tyrosine kinase AXL as well as the leucine rich repeat protein LRRC4C, which in our previous siRNA screen were shown to be required for bacterial infection and in our present study are efficiently internalized upon LLO treatment. It is tempting to speculate that during host colonization, internalization of infection-promoting factors might give early invading bacteria an advantage to secure their niche, a potentially important concept that should be evaluated in the context of competing pathogens under physiological conditions. Other molecules like the Na^{+}-dependent amino acid transporter SLC6A15 or the endoplasmic reticulum degradation enhancer EDEM3, which in our previous siRNA screen were shown to inhibit infection, are translocated to the cell surface location and increased in abundance upon LLO treatment in our present study. These molecules are therefore associated to novel signaling cascades that block bacterial entry into host cells.

We were particularly interested in proteins which were translocated to the surface upon LLO cell exposure and which contribute positively to the *L. monocytogenes* infection process. Among these, we identified a cluster of ten proteins which are functionally associated with the endoplasmic reticulum, late endosomes/lysosomes and exosomes. We validated our CSC results by monitoring the translocation of the protein LAMP-1 to the surfaceome using flow cytometry, fixed-cell fluorescence microscopy and live-cell spinning disk confocal microscopy. Our results confirmed that LLO induces the cell surface translocation of LAMP-1 in a concentration-, time- and Ca^{2+}-dependent manner, which correlates with the concomitant export of exosomes and the release of lysosomal contents in the extracellular space. Intact *L. monocytogenes* also produce this LAMP-1 translocation to bacterial entry foci in a Ca^{2+}-dependent manner, and by perturbing the function of late endosomes/lysosomes we do not only show that these compartments are the donor pools of LAMP-1, we also demonstrate that perturbation of this translocation inhibits *L. monocytogenes* entry.

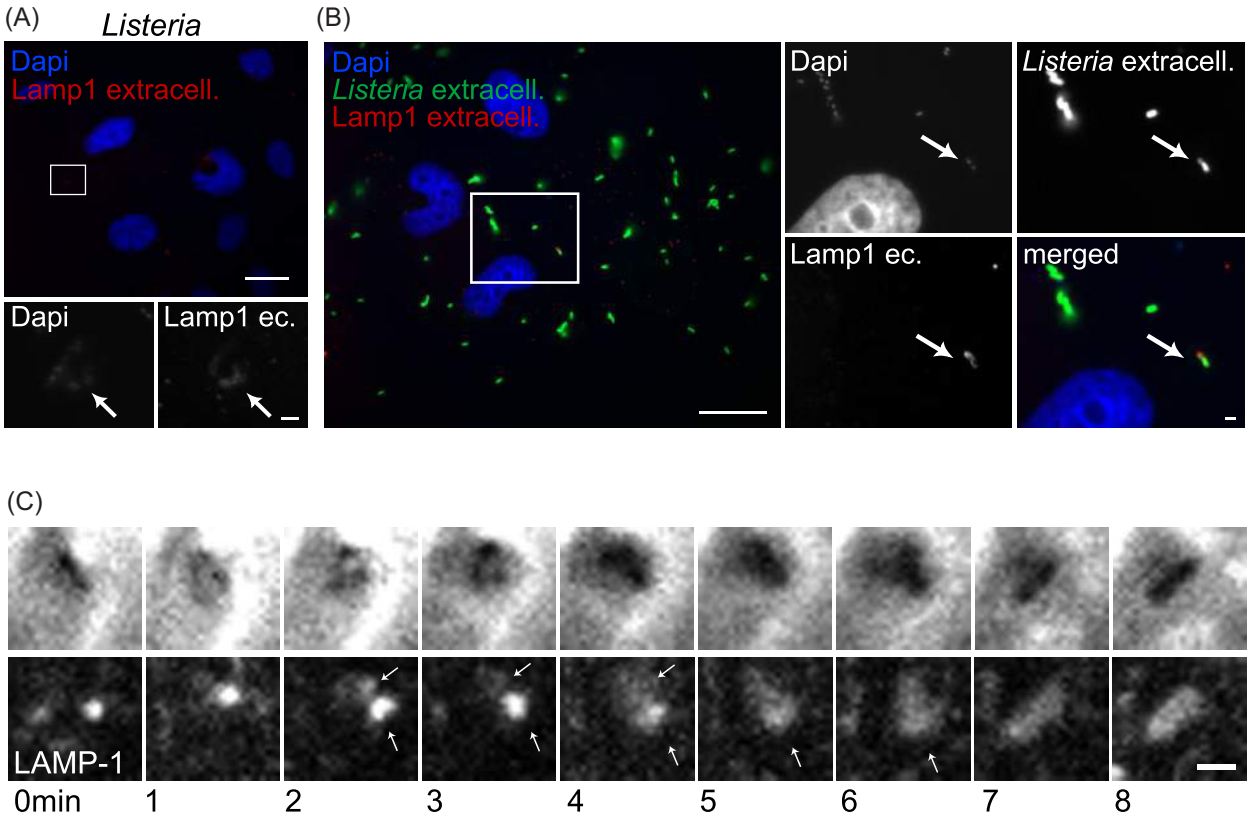

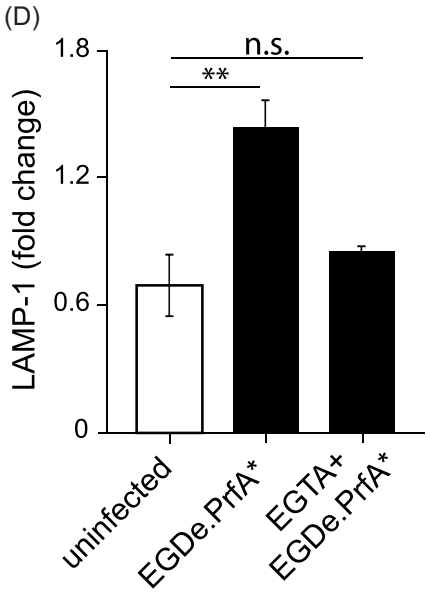

Figure 4. Late endosomes/lysosomes fuse with the plasma membrane at the L. *monocytogenes* entry site during invasion. **A,** HeLa cells grown on coverslips were infected with *L. monocytogenes* EGDe.PrfA* for 20 min. To synchronize infection cells were centrifuged for 5 min at room temperature after inoculation. Cells were then fixed, stained for extracellular LAMP-1 and then permeabilized and stained for DNA allowing to visualize total bacteria using Dapi. The arrow points towards a group of LAMP-1 positive bacteria Bar: 10 μm (magnification bar: 1 μm). **B,** Cells were infected as in A and stained for extracellular LAMP-1 and extracellular bacteria without permeabilization. Subsequently cells were permeabilized and stained for total DNA. The arrow points towards a LAMP-1-positive extracellular *L. monocytogenes* in the process of cell invasion. Bar: 10 μm (magnification bar: 1 μm). **C,** HeLa cells grown on 35 mm imaging dishes and transfected with EGFP-LAMP-1 were infected with *L. monocytogenes* EGDe.PrfA* and centrifuged for 5 min at room temperature to synchronize infection before image acquisition in a spinning disk microscope at 37°C. Upper panel: phase contrast channel; lower panel: GFP channel. Arrows point to LAMP-1-positive vesicles that associate with- and seemingly fuse with the *L. monocytogenes*-containing vacuole during the course of bacterial invasion. Bar: 1 μm. **D,** HeLa cells were pretreated for 20 min with 20mM HEPES or 10 mM EGTA and 20mM HEPES and left uninfected or infected for 20 min with *L. monocytogenes* EGDe.PrfA* in the presence of the different treatments. Following this, cells were detached, fixed and fluorescently stained for surface accessible LAMP-1 in the absence of permeabilization. The fluorescent signal was measured by flow cytometry. Geometric mean of fluorescence intensity was normalized to the average of all samples. Bars represent the mean and SEM of three independent experiments.

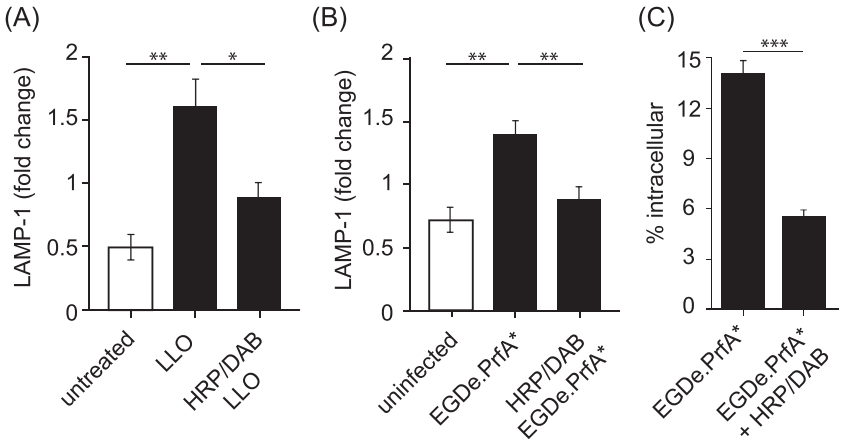

Figure 5. Perturbation of late endosomal/lysosomal compartments blocks LAMP-1 translocation and reduces *L. monocytogenes* invasion. HeLa cells were let untreated or were incubated with 5 mg/ml HRP for 1.5 h followed by 30 min of chase in the absence of the enzyme and 30 min of lysosomal/late endosomal cross-linking by DAB/H_2O_2 exposure on ice. Cells were then treated with mock DMEM or treated with 1 nM LLO in DMEM for 20 min (**A**) or infected for 20 min with *L. monocytogenes* EGDe.PrfA* (**B**). After fixation cells were stained for LAMP-1 and analyzed by flow cytometry. Geometric mean of fluorescence intensity was normalized to the average of all samples. Mean and SEM of three independent experiments are presented (Student's *t*-test: *, $p < 0.05$). **C**, Cells treated with HRP and DAB/H_2O_2 (as in A and B) were infected with *L. monocytogenes* EGDe.PrfA* for 40 min and extracellular bacteria were stained differentially (A). Results represent the average intracellular bacteria (% of total) + /- standard error of the mean (Student's *t*-test: ***, $p < 0.001$).

Targeting of lysosomal compartments to the plasma membrane of fibroblasts and epithelial cells has been reported as a Ca^{2+}-dependent repair mechanism triggered upon mechanical wounding aggressions, including membrane disruption by the pore-forming toxin streptolysin O (Rodríguez *et al.* 1997; Reddy, Caler and ANDREWS 2001), a process dependent on Synaptotagmin VII (Rao 2004; Czibener *et al.* 2006). Membrane injury by *Salmonella enterica*, a bacterial pathogen that harbors a type III secretion system that induces Ca^{2+}-influx, activates this repair mechanism which limits bacterial intracellular growth (Roy *et al.* 2004). Interaction of lysosomes with invading pathogens has also been described in the case of the parasites *Trypanosoma cruzi* (Tardieux *et al.* 1992; Kima, Burleigh and Andrews 2000; Fernandes *et al.* 2011) and *Leishmania donovani* (Forestier *et al.* 2011); in the particular case of *T. cruzi*, host cell membrane wounding by the parasite flagellum induces a Ca^{2+} influx which mobilizes LAMP-1 positive lysosomes to the plasma membrane: secretion of an acid sphingomyelinase from lysosomes to the outer leaflet of the plasma membrane induces the production of ceramide to promote membrane repair, and *T. cruzi* takes advantage of ceramide-rich microdomains to favor the formation of its parasitophorous vacuole (Fernandes *et al.* 2011). The results we report in this manuscript are highly reminiscent of the lysosome-based membrane repair mechanisms described in previous works and represent, to our knowledge, the first description of late endosomal/lysosomal compartments exocytosis favoring the entry of a bacterial pathogen.

As mentioned above, LLO has been previously reported to promote Ca^{2+} entry within epithelial cells and this influx was shown to favor bacterial entry, but the molecular mechanism(s) regulated by this ion during *L. monocytogenes* invasion were not characterized at the time (Dramsi and Cossart 2003). LLO-induced Ca^{2+} influx has also been shown to induce fragmentation of mitochondria and it was proposed to indirectly affect bacterial infection by modulating mitochondrial function (Stavru *et al.* 2011). More recently, it has been demonstrated that LLO promotes entry by a dynamin- and F-actin-dependent but InlA/InlB- and clathrin-independent pathway that induces membrane extensions and particle engulfment (Vadia *et al.* 2011; Vadia and Seveau 2014). Our results are in agreement with these previous observations and indicate therefore that late endosomes/lysosomes participate to this LLO-dependent entry process, and suggest that LLO synergizes with the InlB-dependent pathway to promote efficient plasma membrane remodeling during the early *L. monocytogenes* invasion steps. Along this line, it is interesting to note that we also identified an increase in the plasma membrane levels of LAMP-1 upon cell exposure to purified InlB, which correlate with a recently described role for host cell exocytosis in InlB-mediated internalization (Van Ngo *et al.* 2017), confirming therefore a synergy between the InlB- and the LLO-dependent internalization pathway.

In this context, it is important to mention that LAMP-1 surface translocation can also occur through an unconventional endo-secretory pathway that implicates a population of early endocytic compartments and requires in part the function of the clathrin adaptor AP-1 (Laulagnier *et al.* 2011). Remarkably, AP-1 fosters optimal phagocytosis in macrophages (Braun *et al.* 2004; 2007), participates in the polarized exocytosis of LAMP-2-positive lysosomes in epithelial cells during membrane repair (Xu *et al.* 2012), and has been also implicated in *L. monocytogenes* internalization through an InlB-dependent invasion pathway (Pizarro-Cerdá *et al.* 2007). The investigation of the molecular intersection between these signaling cascades during *L. monocytogenes* infection represents a promising research avenue to explore in the future.

SUPPLEMENTARY DATA

Supplementary data are available at *FEMSPD* online.

AUTHOR CONTRIBUTIONS

A. Kühbacher, K. Novel, B. Wollscheid and J. Pizarro-Cerdá designed research; A. Kühbacher, K. Novel, J.J. Quereda, M. Sachse, M. Moya-Nilges and J. Pizarro-Cerdá performed experiments; A. Kühbacher, K. Novel, B. Wollscheid and J. Pizarro-Cerdá analyzed the data; and A. Kühbacher, P. Cossart and J. Pizarro-Cerdá wrote the paper.

ACKNOWLEDGEMENTS

We thank Jean Gruenberg for the gift of anti-LBPA antibodies and Pierre-Yves Lozach for the EGFP-LAMP-1 plasmid. This work received financial support from the Institut Pasteur (PTR 521), Institut National de la Santé et de la Recherche Médicale (Unité 604), Institut National de la Recherche Agronomique (Unité Sous Contrat 2020), Fondation Louis Jeantet, European Research Council Advanced (Grant BacCellEpi) and Agence Nationale pour la Recherche. Support was also provided by the Swiss Science National Foundation (to B.W.) and the Scgrant 51RT 0˙126008 for the Research and Technology Development (RTD) project InfectX in the frame of SystemsX.ch, the Swiss Initiative for Systems Biology (to K.N. and B.W.). P.C. is a Howard Hughes Medical Institute Senior International Research Scholar. A.K. was a recipient of a scholarship from the Pasteur-Paris University International Doctoral Program/Institut Carnot Maladies Infectieuses.

Conflict of interest. None declared.

REFERENCES

Bierne H, Gouin E, Roux P *et al.* A role for cofilin and LIM kinase in Listeria-induced phagocytosis. *J Cell Biol* 2001;**155**:101–12.

Bierne H, Miki H, Innocenti M *et al.* WASP-related proteins, Abi1 and Ena/VASP are required for Listeria invasion induced by the Met receptor. *J Cell Sci* 2005;**118**:1537–47.

Bonazzi M, Kühbacher A, Toledo-Arana A *et al.* A common Clathrin-mediated machinery co-ordinates cell-cell adhesion and bacterial internalization. *Traffic* 2012;**13**:1653–66.

Bonazzi M, Vasudevan L, Mallet A *et al.* Clathrin phosphorylation is required for actin recruitment at sites of bacterial adhesion and internalization. *J Cell Biol* 2011;**195**:525–36.

Braun V, Deschamps C, Raposo G *et al.* AP-1 and ARF1 control endosomal dynamics at sites of FcR–mediated phagocytosis. *MBoC* 2007;**18**:4921–31.

Braun V, Fraisier V, Raposo G *et al.* TI-VAMP/VAMP7 is required for optimal phagocytosis of opsonised particles in macrophages. *EMBO J* 2004;**23**:4166–76.

Clough T, Key M, Ott I *et al.* Protein Quantification in Label-Free LC-MS Experiments. *J Proteome Res* 2009;**8**:5275–84.

Czibener C, Sherer NM, Becker SM *et al.* Ca2+ and synaptotagmin VII-dependent delivery of lysosomal membrane to nascent phagosomes. *J Cell Biol* 2006;**174**:997–1007.

Dramsi S, Cossart P. Listeriolysin O-mediated calcium influx potentiates entry of Listeria monocytogenes into the human Hep-2 epithelial cell line. *Infect Immun* 2003;**71**:3614–8.

Eng JK, McCormack AL, Yates JR. An approach to correlate tandem mass spectral data of peptides with amino acid sequences in a protein database. *J Am Soc Mass Spectrom* 1994;**5**:976–89.

Fernandes MC, Cortez M, Flannery AR *et al.* Trypanosoma cruzi subverts the sphingomyelinase-mediated plasma membrane repair pathway for cell invasion. *J Exp Med* 2011;**208**:909–21.

Forestier C-L, Machu C, Loussert C *et al.* Imaging host cell-leishmania interaction dynamics implicates parasite motility, lysosome recruitment, and host cell wounding in the infection process. *Cell Host Microbe* 2011;**9**:319–30.

Futter CE, Pearse A, Hewlett LJ *et al.* Multivesicular endosomes containing internalized EGF-EGF receptor complexes mature and then fuse directly with lysosomes. *J Cell Biol* 1996;**132**:1011–23.

Gaillard JL, Berche P, Frehel C *et al.* Entry of L. monocytogenes into cells is mediated by internalin, a repeat protein reminiscent of surface antigens from gram-positive cocci. *Cell* 1991;**65**:1127–41.

Gessain G, Tsai YH, Travier L *et al.* PI3-kinase activation is critical for host barrier permissiveness to Listeria monocytogenes. *J Exp Med* 2015;**212**:165–83.

Glomski IJ, Decatur AL, Portnoy DA. Listeria monocytogenes mutants that fail to compartmentalize listerolysin O activity are cytotoxic, avirulent, and unable to evade host extracellular defenses. *Infect Immun* 2003;**71**:6754–65.

Gouin E, Welch MD, Cossart P. Actin-based motility of intracellular pathogens. *Curr Opin Microbiol* 2005;**8**:35–45.

Hamon MA, Batsché E, Régnault B *et al.* Histone modifications induced by a family of bacterial toxins. *Proc Natl Acad Sci* 2007;**104**:13467–72.

Hamon MA, Cossart P. K+ Efflux Is Required for Histone H3 Dephosphorylation by Listeria monocytogenes Listeriolysin O and Other Pore-Forming Toxins. *Infect Immun* 2011;**79**:2839–46.

Hofmann A, Bausch-Fluck D, Wollscheid B. CSC technology: selective labeling of glycoproteins by mild oxidation to phenotype cells. *Methods Mol Biol* 2013;**951**:33–43.

Ireton K, Payrastre B, Chap H *et al.* A role for phosphoinositide 3-kinase in bacterial invasion. *Science* 1996;**274**:780–2.

Ireton K, Payrastre B, Cossart P. The Listeria monocytogenes protein InlB is an agonist of mammalian phosphoinositide 3-kinase. *J Biol Chem* 1999;**274**:17025–32.

Keller A, Eng J, Zhang N *et al.* A uniform proteomics MS/MS analysis platform utilizing open XML file formats. *Mol Syst Biol* 2005;**1**:E1–E8.

Kima PE, Burleigh B, Andrews NW. Surface-targeted lysosomal membrane glycoprotein-1 (Lamp-1) enhances lysosome exocytosis and cell invasion by Trypanosoma cruzi. *Cell Microbiol* 2000;**2**:477–86.

Kühbacher A, Cossart P, Pizarro-Cerdá J. Internalization assays for Listeria monocytogenes. *Methods in Molecular Biology*. Vol **1157**. New York, NY: Springer New York, 2014, 167–78.

Kühbacher A, Dambournet D, Echard A *et al.* Phosphatidylinositol 5-phosphatase oculocerebrorenal syndrome of Lowe protein (OCRL) controls actin dynamics during early steps of Listeria monocytogenes infection. *J Biol Chem* 2012;**287**:13128–36.

Kühbacher A, Emmenlauer M, Rämö P *et al.* Genome-Wide siRNA Screen Identifies Complementary Signaling Pathways Involved in ListeriaInfection and Reveals Different Actin Nucleation Mechanisms during ListeriaCell Invasion and Actin Comet Tail Formation. *mBio* 2015;**6**:e00598–15.

Laulagnier K, Schieber NL, Maritzen T *et al.* Role of AP1 and Gadkin in the traffic of secretory endo-lysosomes. *MBoC* 2011;**22**:2068–82.

Lecuit M. Human listeriosis and animal models. *Microbes Infect* 2007;**9**:1216–25.

Lozach P-Y, Kühbacher A, Meier R *et al.* DC-SIGN as a Receptor for Phleboviruses. *Cell Host Microbe* 2011;**10**:75–88.

Malet JK, Impens F, Carvalho F *et al.* Rapid Remodeling of the Host Epithelial Cell Proteome by the Listeriolysin O (LLO) Pore-forming Toxin. *Mol Cell Proteomics* 2018;**17**:1627–36.

Mengaud J, Ohayon H, Gounon P *et al.* E-cadherin is the receptor for internalin, a surface protein required for entry of L. monocytogenes into epithelial cells. *Cell* 1996;**84**:923–32.

Michel E, Reich KA, Favier R *et al.* Attenuated mutants of the intracellular bacterium Listeria monocytogenes obtained by

single amino acid substitutions in listeriolysin O. *Mol Microbiol* 1990;**4**:2167–78.
Pizarro-Cerdá J, Bonazzi M, Cossart P. Clathrin-mediated endocytosis: What works for small, also works for big. *Bioessays* 2010;**32**:496–504.
Pizarro-Cerdá J, Charbit A, Enninga J *et al.* Manipulation of host membranes by the bacterial pathogens Listeria, Francisella, Shigella and Yersinia. *Semin Cell Dev Biol* 2016;**60**:1–13.
Pizarro-Cerdá J, Cossart P. Listeria monocytogenes membrane trafficking and lifestyle: the exception or the rule? *Annu Rev Cell Dev Biol* 2009;**25**:649–70.
Pizarro-Cerdá J, Kühbacher A, Cossart P. Entry of Listeria monocytogenes in mammalian epithelial cells: an updated view. *Cold Spring Harbor Perspectives in Medicine* 2012;**2**, DOI: 10.1101/cshperspect.a010009.
Pizarro-Cerdá J, Kühbacher A, Cossart P. Phosphoinositides and host-pathogen interactions. *Biochim Biophys Acta* 2014, DOI: 10.1016/j.bbalip.2014.09.011.
Pizarro-Cerdá J, Lecuit M, Cossart P. Measuring and analysing invasion of mammalian cells by bacterial pathogens: the Listeria monocytogenes system. *Methods Microbiol* 2002;**31**:a010009-.
Pizarro-Cerdá J, Payrastre B, Wang Y-J *et al.* Type II phosphatidylinositol 4-kinases promote Listeria monocytogenes entry into target cells. *Cell Microbiol* 2007;**9**:2381–90.
Quereda JJ, Cossart P, Pizarro-Cerda J. Role of Listeria monocytogenes exotoxins in virulence. In Gopalakrishnakone P, Stiles B, Alape-Giron A *et al.* (eds). *Microbial Toxins*. Dordrecth: Springer, 2016, https://doi.org/10.1007/978-94-007-6725-6_24-1.
Quereda JJ, Rodríguez-Gómez IM, Meza-Torres J *et al.* Reassessing the role of Internalin B in Listeria monocytogenes virulence using the epidemic strain F2365. *Clin Microbiol Infect* 2018:1–14, DOI: 10.1016/j.cmi.2018.08.022.
Rao SK. Identification of SNAREs involved in Synaptotagmin VII-regulated Lysosomal Exocytosis. *J Biol Chem* 2004;**279**:20471–9.
Reddy A, Caler E, ANDREWS N. Plasma membrane repair is mediated by Ca2+-regulated exocytosis of lysosomes. *Cell* 2001;**106**:157–69.
Ribet D, Hamon M, Gouin E *et al.* Listeria monocytogenes impairs SUMOylation for efficient infection. *Nature* 2010;**464**:1192–5.
Rodríguez A, Webster P, Ortego J *et al.* Lysosomes behave as Ca2+-regulated exocytic vesicles in fibroblasts and epithelial cells. *J Cell Biol* 1997;**137**:93–104.
Roy D, Liston DR, Idone VJ *et al.* A process for controlling intracellular bacterial infections induced by membrane injury. *Science* 2004;**304**:1515–8.
Samba-Louaka A, Stavru F, Cossart P. Role for Telomerase in Listeria monocytogenes Infection. *Infect Immun* 2012;**80**:4257–63.
Seveau S, Tham TN, Payrastre B *et al.* A FRET analysis to unravel the role of cholesterol in Rac1 and PI 3-kinase activation in the InlB/Met signalling pathway. *Cell Microbiol* 2007;**9**:790–803.
Seveau S. Role of lipid rafts in E-cadherin- and HGF-R/Met-mediated entry of Listeria monocytogenes into host cells. *J Cell Biol* 2004;**166**:743–53.
Shen Y, Naujokas M, Park M *et al.* InlB-Dependent Internalization of Listeria Is Mediated by the Met Receptor Tyrosine Kinase. *Cell* 2000;**103**:501–10.
Stavru F, Bouillaud F, Sartori A *et al.* Listeria monocytogenes transiently alters mitochondrial dynamics during infection. *Proc Natl Acad Sci USA* 2011;**108**:3612–7.
Stavru F, Cossart P. Listeria infection modulates mitochondrial dynamics. *Commun Integr Biol* 2011;**4**:364–6.
Stavru F, Palmer AE, Wang C *et al.* Atypical mitochondrial fission upon bacterial infection. *Proc Natl Acad Sci* 2013, DOI: 10.1073/pnas.1315784110.
Stoorvogel W, Kleijmeer MJ, Geuze HJ *et al.* The biogenesis and functions of exosomes. *Traffic* 2002;**3**:321–30.
Suárez M, González-Zorn B, Vega Y *et al.* A role for ActA in epithelial cell invasion by Listeria monocytogenes. *Cell Microbiol* 2001;**3**:853–64.
Swaminathan B, Gerner-Smidt P. The epidemiology of human listeriosis. *Microbes Infect* 2007;**9**:1236–43.
Szklarczyk D, Franceschini A, Wyder S *et al.* STRING v10: protein–protein interaction networks, integrated over the tree of life. *Nucleic Acids Res* 2015;**43**:D447–52.
Tardieux I, Webster P, Ravesloot J *et al.* Lysosome recruitment and fusion are early events required for trypanosome invasion of mammalian cells. *Cell* 1992;**71**:1117–30.
Vadia S, Arnett E, Haghighat A-C *et al.* The pore-forming toxin listeriolysin O-mediates a novel entry pathway of L. monocytogenes into human hepatocytes. *PLoS Pathog* 2011;**7**:e1002356.
Vadia S, Seveau S. Fluxes of Ca2+ and K+ are required for the listeriolysin O-dependent internalization pathway of listeria monocytogenes. *Infect Immun* 2014;**82**:1084–91.
Van Ngo H, Bhalla M, Chen D-Y *et al.* A role for host cell exocytosis in InlB-mediated internalisation of Listeria monocytogenes. *Cell Microbiol* 2017;**19**:e12768.
Van Niel G, Raposo G, Candalh C *et al.* Intestinal Epithelial Cells Secrete Exosome-like Vesicles. *Gastroenterology* 2001;**121**:337–49.
Van Troys M, Lambrechts A, David V *et al.* The actin propulsive machinery: The proteome of Listeria monocytogenes tails. *Biochem Biophys Res Commun* 2008;**375**:194–9.
Veiga E, Cossart P. Listeria hijacks the clathrin-dependent endocytic machinery to invade mammalian cells. *Nat Cell Biol* 2005;**7**:894–900.
Veiga E, Guttman JA, Bonazzi M *et al.* Invasive and adherent bacterial pathogens co-opt host clathrin for infection. *Cell Host Microbe* 2007;**2**:340–51.
Wollscheid B, Bausch-Fluck D, Henderson C *et al.* Mass-spectrometric identification and relative quantification of N-linked cell surface glycoproteins. *Nat Biotechnol* 2009;**27**:378–86.
Xu J, Toops KA, Diaz F *et al.* Mechanism of polarized lysosome exocytosis in epithelial cells. *J Cell Sci* 2012;**125**:5937–43.